Journal of Alloys and Compounds 509 (2011) 1841–1847

Contents lists available at ScienceDirect

Journal of Alloys and Compounds

journal homepage: www.elsevier.com/locate/jallcom

Hydrogenation properties of Ti–V–Mn alloys with a BCC structure containing high and low oxygen concentrations

Y. Nakamura*, J. Nakamura, K. Sakaki, K. Asano, E. Akiba

National Institute of Advanced Industrial Science and Technology (AIST), AIST Central-5, 1-1-1 Higashi, Tsukuba, Ibaraki 305-8565, Japan

ARTICLE INFO

Article history:
Received 9 September 2010
Accepted 13 October 2010
Available online 21 October 2010

Keywords:
Hydrogen storage
Alloy
BCC structure
P–C isotherm
Formation enthalpy
Oxygen effect

ABSTRACT

The hydrogenation properties of $Ti_{1.0}V_{1.1}Mn_{0.9}$ alloys with a BCC structure, prepared using two V materials with different oxygen concentrations, were studied. The sample prepared using a conventional-grade V material contained 0.530 mass% of oxygen, and the other sample prepared from a low-oxygen V material contained 0.051 mass% of oxygen. Both samples showed *P–C* isotherms with two plateaus corresponding to formation of monohydrides and dihydrides. The sample with the higher oxygen concentration had an equilibrium pressure for dihydride formation 6.7 times higher than that of the sample with the lower oxygen concentration at 0 °C. There was no significant difference between the two samples with regard to the equilibrium pressure for formation of monohydride or the hydrogen capacity. The formation enthalpies were calculated from the van't Hoff plots: −30.2 kJ/molH_2 and −35.5 kJ/molH_2 for the dihydrides, and −39.7 kJ/molH_2 and −39.8 kJ/molH_2 for the monohydrides. Scanning electron microscopy/energy dispersive X-ray spectroscopy (SEM–EDX) and X-ray diffraction (XRD) indicated that the sample with the higher oxygen concentration contained a Ti-rich secondary phase, which caused changes in the composition and in the lattice parameter of the main phase. These results indicated that increasing the oxygen concentration altered the hydrogenation properties as a result of (1) the effect of oxygen solved in the main phase on hydrogen occupation and (2) a composition change resulting from secondary phase formation.

© 2010 Elsevier B.V. All rights reserved.

1. Introduction

Hydrogen storage materials have attracted great interest for a use in fuel cell vehicles. Among these materials, metal-based materials, so-called *metal hydrides*, generally have the advantages of a large capacity per volume, and favorable kinetics and cyclic stability, but the disadvantage of a low capacity per weight. Ti- or V-based solid solution alloys with a BCC structure are known to have the largest reversible hydrogen capacity at around room temperature, ca. 3 mass% [1–3]. Mori et al. demonstrated that a high-pressure tank of about 200 kg and 100 L containing this type of material can store 5 kg of hydrogen [4].

The hydrogenation properties of $Ti_{1.0}V_{1.1}Mn_{0.9}$ alloy were first reported by Iba and Akiba in 1995 [5]. This was the first report to show that Ti- or V-based solid solution alloys with a BCC structure can store more than 2 mass% of hydrogen reversibly at around room temperature. They only reported a desorption *P–C* isotherm, which appeared to have only one plateau. Some of the authors investigated phase transformations of Ti–V–Mn alloys with similar compositions along the *P–C* isotherms [6]. $Ti_{1.0}V_{1.1}Mn_{0.9}$ showed two clear plateaus in the *P–C* isotherms during absorption: the plateau at a lower pressure corresponds to transformation from a solid solution phase ($Ti_{1.0}V_{1.1}Mn_{0.9}H_{\sim0.5}$) to a monohydride phase ($Ti_{1.0}V_{1.1}Mn_{0.9}H_{\sim1}$), and the plateau at a higher pressure corresponds to transformation from the monohydride phase to a dihydride phase ($Ti_{1.0}V_{1.1}Mn_{0.9}H_{\sim2}$). The desorption *P–C* isotherm also showed two plateaus, but they were not clearly separated because their pressures were so similar. The structures of the two hydrides prepared with deuterium were studied by powder neutron diffraction, which revealed that the monohydride and the dihydride have a pseudo-cubic NaCl structure and a CaF_2 structure, respectively [7]. The equilibrium pressures of the two plateaus strongly depend on the alloy composition and the lattice parameter [8]. A Ti-rich composition showed a lower plateau pressure, and a Mn-rich composition showed a higher plateau pressure. Only limited compositions of around $Ti_{1.0}V_{1.1}Mn_{0.9}$ showed two plateaus in the *P–C* isotherms under the experimental conditions used [8]. In that series of studies, thermodynamic parameters such as formation enthalpy and entropy were not reported because it was difficult to obtain reproducible *P–C* isotherms with flat plateaus, which are needed for making reliable van't Hoff plots. Our

* Corresponding author at: Hydrogen Energy Group, Energy Technology Research Institute, National Institute of Advanced Industrial Science and Technology (AIST), AIST Central-5, 1-1-1 Higashi, Tsukuba, Ibaraki 305-8565, Japan.
Tel.: +81 29 861 4543; fax: +81 29 861 4543.
E-mail address: yumiko.nakamura@aist.go.jp (Y. Nakamura).

0925-8388/$ – see front matter © 2010 Elsevier B.V. All rights reserved.
doi:10.1016/j.jallcom.2010.10.059

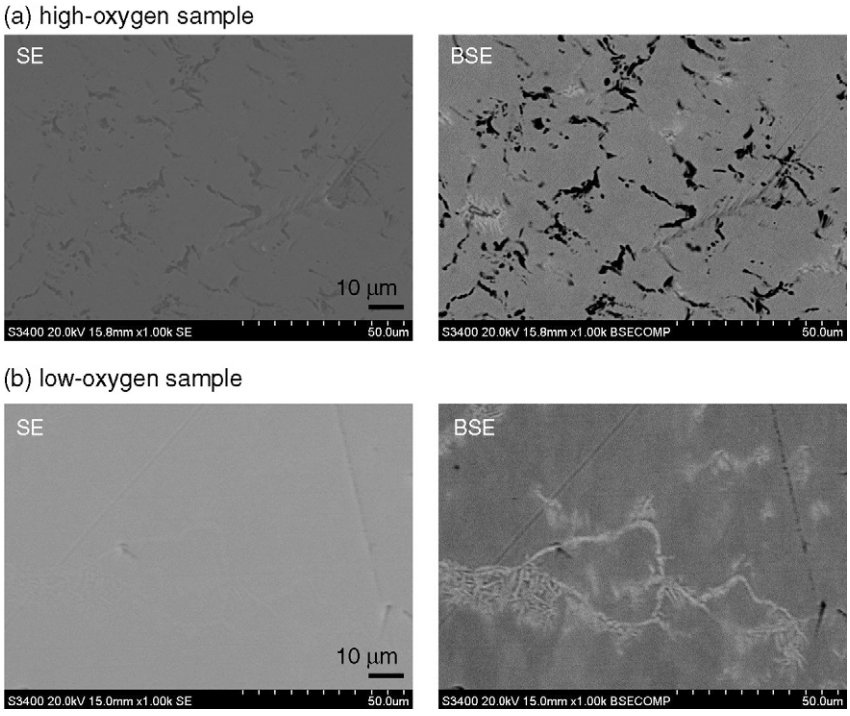

Fig. 1. SEM images of two $Ti_{1.0}V_{1.1}Mn_{0.9}$ samples with high (a) and low (b) oxygen concentrations. SE: secondary electron images; BSE: back-scattered electron images. Note that image (b) focused on an area containing a larger than average fraction of the secondary phase.

subsequent study suggested that the lack of reproducibility was partly attributable to variations in the amounts of oxygen contained in the samples.

V-based BCC alloys basically have hydrogenation properties similar to V metal. The hydrogenation properties of V, including the *P–C* isotherms, were first reported by Reilly and Wiswall [9]. They indicated that even a small amount of oxygen in V affects the *P–C* isotherms, particularly the dissociation pressure, based on results with high-purity, zone-refined V (oxygen content: 112 ppm) and commercial-grade V (oxygen content: 430 ppm). Tsukahara et al. reported that the oxygen content in V strongly affected both hydrogen content and equilibrium pressure [10]. They examined V metals with oxygen concentrations of 200 ppm and 4000 ppm, and V_3Ti-based BCC alloys with oxygen concentrations ranging from 600 ppm to 9000 ppm. For both series, the hydrogen capacities decreased and the plateau pressure increased with oxygen concentration. As most commercial-grade V materials contain several hundred ppm or more of oxygen, it is expected that the samples used in most previous studies, including our work [6–8], contained this level of oxygen, and that the results were affected by the presence of oxygen. It is worth examining how a difference in oxygen concentration affects the hydrogenation properties of BCC alloys containing V as one of the constituents.

This paper reports the hydrogenation properties of Ti–V–Mn alloys showing two plateaus in their *P–C* isotherms, focusing on the effects of oxygen content. Two alloy samples were prepared using V materials with two different oxygen concentrations. The values of the formation and dissociation enthalpies (ΔH) and entropies (ΔS) for the monohydride and the dihydride were evaluated for each sample from the van't Hoff plot. Morphology and local compositions were examined using scanning electron microscopy/energy dispersive X-ray spectroscopy (SEM–EDX). The lattice parameters of the alloy phases and the hydride phases were obtained by powder X-ray diffraction (XRD). The causes of the differences in the hydrogenation properties of the two samples will be discussed with respect to the results of chemical analyses and XRD studies.

2. Experimental

Two alloy samples of $Ti_{1.0}V_{1.1}Mn_{0.9}$ were prepared by arc melting from two different V materials and common Ti and Mn materials. The oxygen concentrations of the two V materials were analyzed by the inert gas fusion–IR method (TCH-600; LECO): 1.22 mass% for one V material (conventional grade; purity >99.9%), and 0.0111 mass% for the other V material (low-oxygen grade; purity >99.9%). The prepared samples contained 0.530 mass% and 0.051 mass% oxygen, respectively. Their morphology and compositions were analyzed by SEM (S3400-N, Hitachi) and EDX spectroscopy (GENESIS 2000H, EDAX).

The sample ingots were crushed into particles of a few millimeters for measuring the *P–C* isotherms. The particles were sealed in a stainless steel container and the container was evacuated at 120 °C using a turbo molecular pump. After cooling to room temperature, the samples were pressurized by hydrogen gas up to 5 MPa. The evacuation and hydrogenation were repeated three times. The *P–C* isotherms at temperatures between 0 °C and 80 °C were measured. The samples were evacuated at 500 °C for complete dehydrogenation before every absorption measurement.

Powder XRD data of the alloys before hydrogenation, the monohydrides, and the dihydrides were obtained using an X-ray diffractometer (RINT-2500V, Rigaku) equipped with a rotating anode X-ray source. CuKα radiation was used for diffraction. The monohydrides and dihydrides were prepared by hydrogenating the alloy samples along the *P–C* isotherms, followed by deactivation of the surface with acetone. Each sample was confirmed to keep the corresponding hydride phase in air for at least a couple of days. Their metal lattice structures were determined by the Rietveld method using Rietan-2000 [11,12].

3. Results

3.1. Phase relations in the prepared samples

Fig. 1 shows SEM images obtained for the two $Ti_{1.0}V_{1.1}Mn_{0.9}$ samples with high and low oxygen concentrations (denoted below by "high-oxygen sample" and "low-oxygen sample", respectively). The composition of each phase, obtained by EDX analysis, is listed in Table 1. The high-oxygen sample contained a Ti-rich phase, observed as dark areas in the image (Fig. 1a). This phase contained 72–92% Ti. The area fraction of this phase was estimated at around 5% from the back-scattered electron (BSE) image. A smaller fraction of a V-poor phase was also observed as brighter areas in the BSE image. The average composition of the main phase

Table 1
Compositions of constituent phases in the prepared $Ti_{1.0}V_{1.1}Mn_{0.9}$ samples obtained from SEM-EDX analysis. The listed values were obtained from three point analyses for each phase.

Samples	Phase	Ti (at.%)	V (at.%)	Mn (at.%)
	Target composition	33.3	36.7	30.0
High-oxygen	Main phase	29.6–30.8	41.3–42.0	27.9–28.8
	Ti-rich phase	72–92	4–14	3–13
Low-oxygen	Main phase	32.6–34.3	35.8–37.6	29.7–29.9
	V-poor phase	38.0–41.2	23.8–27.6	30.3–38.1

was $Ti_{0.9}V_{1.2}Mn_{0.9}$, indicating that formation of the Ti-rich phase resulted in a decrease in Ti concentration in the main phase. In contrast, the low-oxygen sample contained little Ti-rich phase, but a larger fraction of dendrites and surrounding areas were observed as brighter areas in the BSE image (Fig. 1b). Rough estimations from several images showed that the average fraction of the brighter areas was around 10%. EPMA mapping indicated that the brighter areas had V-poor compositions. The main phase and the V-poor areas do not have clear boundaries. The average composition of the main phase agreed with the target composition, $Ti_{1.0}V_{1.1}Mn_{0.9}$, and that of the V-poor areas was $Ti_{1.2}V_{0.8}Mn_{1.0}$.

3.2. *P–C* isotherms and thermodynamic parameters

Figs. 2 and 3 show the *P–C* isotherms of $Ti_{1.0}V_{1.1}Mn_{0.9}$ for the high- and low-oxygen samples, respectively. The high-oxygen sample showed isotherms with two plateaus similar to those previously reported [6]. The low-oxygen sample showed a similar shape of isotherms but with different plateau pressures from the high-oxygen sample: the equilibrium pressure for the lower-pressure plateau (denoted below by "lower plateau") was almost the same, but the pressure for the higher-pressure plateau (denoted below by "higher plateau") was apparently lower than that observed for the high-oxygen sample. The difference in absorption pressure for the higher plateau was significant: 0.03 MPa for the low-oxygen sample and 0.2 MPa for the high-oxygen sample at 0 °C. In contrast, only a small difference was observed in the desorption pressures. These differences resulted in a significant difference in hysteresis between the two samples. In the high-oxygen sample in particular, the plateaus were sloping on the higher hydrogen content side but not on the other side.

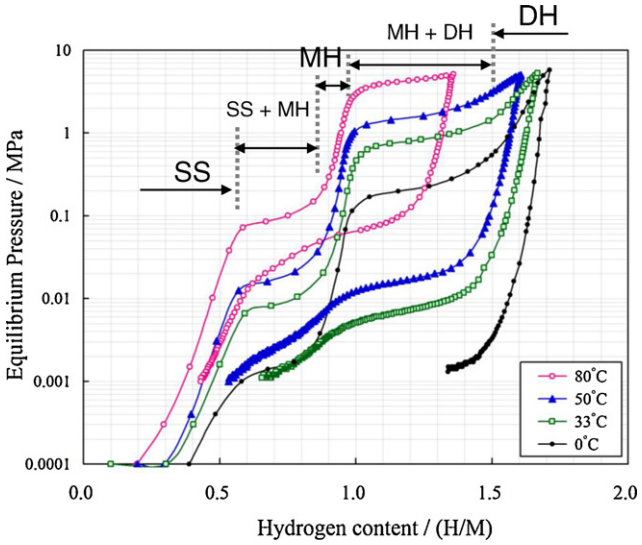

Fig. 2. *P–C* isotherms of $Ti_{1.0}V_{1.1}Mn_{0.9}$ with the higher oxygen concentration. SS, MH, and DH indicate the phases appearing in each region. SS: solid solution phase; MH: monohydride phase; DH: dihydride phase.

Enthalpies and entropies of formation and dissociation of the two hydrides were evaluated from the van't Hoff plots (Fig. 4 and Table 2). Reasonable linear relationships were obtained in the van't Hoff plot other than for dissociation of the monohydride. There was a significant difference between the two samples for the formation enthalpies (ΔH_f) of the dihydride, although little difference was observed in the ΔH_f values for the monohydride, as expected from the observed *P–C* isotherms. The difference between the two samples with reference to the dissociation enthalpy (ΔH_d) of the dihydride was only about 60% of the difference with reference to

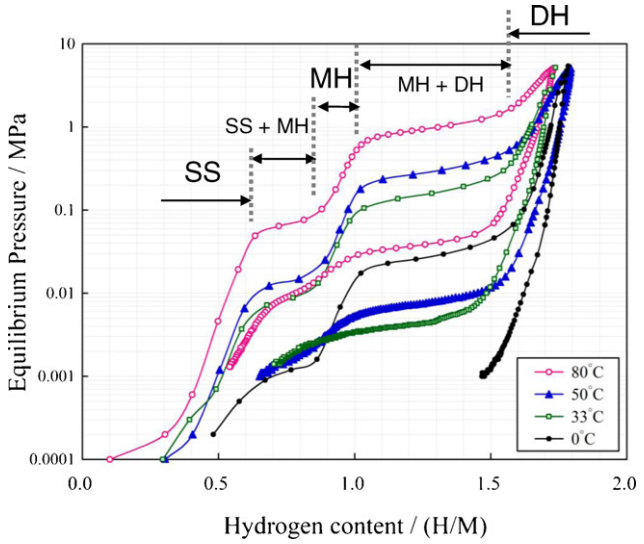

Fig. 3. *P–C* isotherms of $Ti_{1.0}V_{1.1}Mn_{0.9}$ with the lower oxygen concentration. SS, MH, and DH indicate the phases appearing in each region. SS: solid solution phase; MH: monohydride phase; DH: dihydride phase.

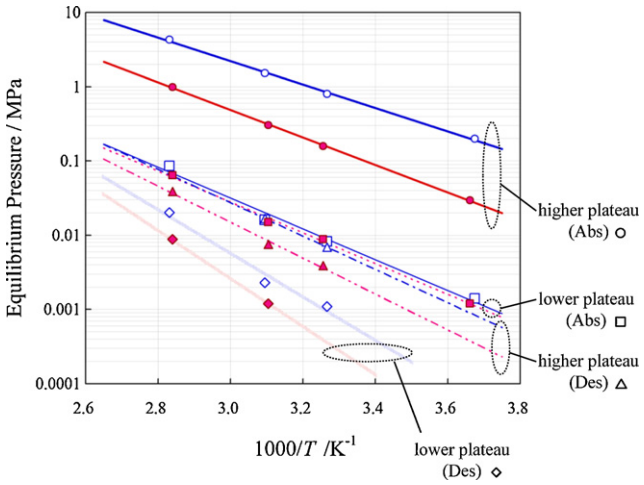

Fig. 4. van't Hoff plots of $Ti_{1.0}V_{1.1}Mn_{0.9}$ with high and low oxygen concentrations. Open symbols: high-oxygen sample; closed symbols: low-oxygen sample. The lines were obtained by least mean squares approximation.

Table 2
Enthalpies and entropies for formation and dissociation of monohydride and dihydride of $Ti_{1.0}V_{1.1}Mn_{0.9}$ (ΔH_f: formation enthalpy, ΔS_f: formation entropy, ΔH_d: dissociation enthalpy, ΔS_d: dissociation entropy).

Samples	ΔH_f (kJ/molH_2)	ΔS_f (J/molH_2/K)	ΔH_d (kJ/molH_2)	ΔS_d (J/molH_2/K)
(a) Formation and dissociation of dihydride				
High-oxygen	−30.2	−116	43.1	118
Low-oxygen	−35.5	−120	46.5	124
Samples	ΔH_f (kJ/molH_2)	ΔS_f (J/molH_2/K)	ΔH_d[a] (kJ/molH_2)	ΔS_d[a] (J/molH_2/K)
(b) Formation and dissociation of monohydride				
High-oxygen	−39.7	−110	~57	~147
Low-oxygen	−39.8	−109	~63	~158

[a] These values are less accurate than the others because of larger deviations from the linear relation in the van't Hoff plot (for the high-oxygen sample), or because of fewer data points (for the low-oxygen sample).

ΔH_f. It was difficult to obtain reliable values of ΔH_d and ΔS_d of the monohydride because the corresponding plateau was not clear in the *P–C* isotherms. Further investigation is needed to clarify the differences in these two values between the two samples.

The hydrogen content at 0 °C and 5 MPa was 1.72 H/M (H/M: atomic ratio of hydrogen and metal) for the high-oxygen sample and 1.79 H/M for the low-oxygen sample. The phase relations observed in the absorption are indicated in Fig. 5. Even though the boundaries are not clear in the high-oxygen sample because of the sloping plateaus, the figure shows that, on the whole, there are no significant differences between the two samples. Looking at the details, the high-oxygen sample shows narrower regions for the solid solution and monohydride phases, but a wider plateau where the solid solution and the monohydride coexist.

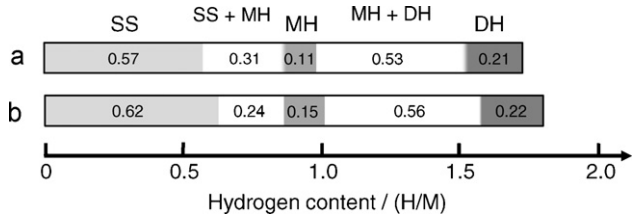

Fig. 5. Phase relations in the absorption *P–C* isotherms: (a) high-oxygen sample, (b) low-oxygen sample. The values show the widths of the regions in H/M.

3.3. XRD of alloy and hydride phases

XRD patterns for the alloy, the monohydride, and the dihydride prepared with the low-oxygen V material are shown in Fig. 6. The patterns were similar to those in our previous report [6], where the samples were prepared with a conventional-grade V material. The metal lattice deformed from BCC to BCT in formation of the monohydride, and then to FCC in formation of the dihydride. The BCT lattice can be taken as a pseudo-cubic FCC lattice, the c' axis of which is shorter than the a' axis by 5–9% when we take the axes as $a' = \sqrt{2}(a_{BCT})$, $c' = c_{BCT}$. Lattice parameters of the three phases prepared with the high- and low-oxygen samples are listed in Table 3.

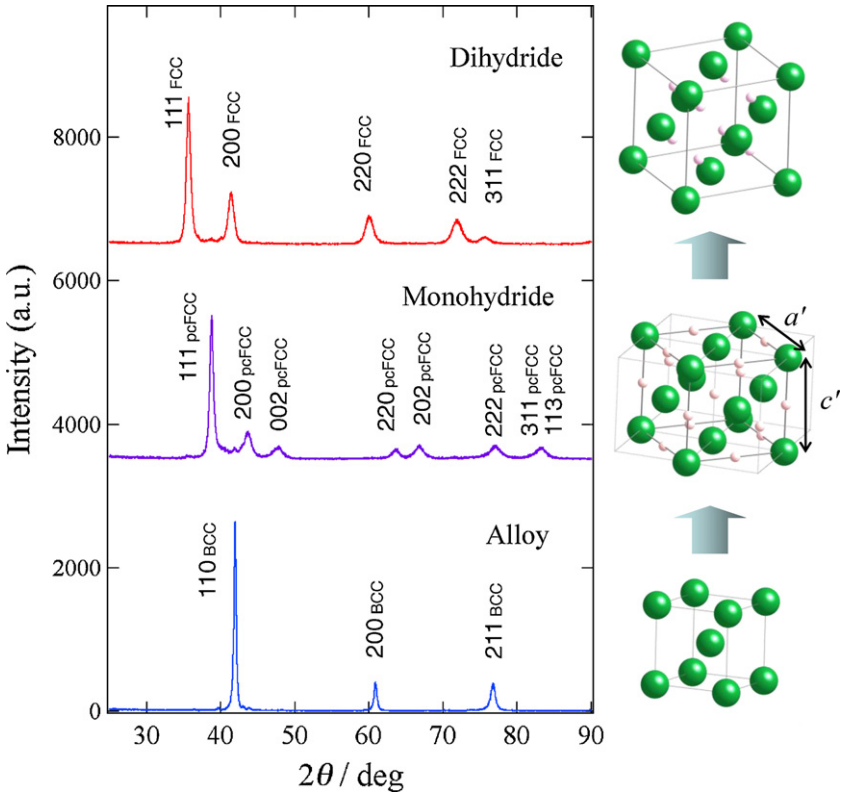

Fig. 6. Powder X-ray diffraction patterns of the alloy (BCC), the monohydride (pseudo-cubic FCC), and the dihydride phases (FCC) for low-oxygen $Ti_{1.0}V_{1.1}Mn_{0.9}$. The refined lattice parameters are listed in Table 3 (sample lot: low-oxygen #1).

Table 3
Lattice parameters for the alloy, monohydride and dihydride of $Ti_{1.0}V_{1.1}Mn_{0.9}$ with high- and low-oxygen concentrations.

Phase [structure]	Sample lot	Hydrogen content (H/M)[a]	a (Å)	c (Å)	c'/a'[b]	
Alloy [BCC]	High-oxygen					
	#1	0	3.0290(2)	–	–	This study[c]
	#2	0	3.0280(1)			Ref. [6]
	Low-oxygen					
	#1	0	3.0389(1)	–	–	This study[c]
	#2	0	3.0383(2)			This study
Monohydride [BCT (a, c) or pseudo-cubic FCC (a', c')]	High-oxygen					
	#1	0.88	2.8966(6)	3.846(1)	0.940	This study[c]
	#2	0.93	2.8808(6)	3.8989(8)	0.957	Ref. [6]
	Low-oxygen					
	#1	0.83	2.9256(5)	3.7983(9)	0.918	This study[c]
	#2	0.87	2.9330(8)	3.787(1)	0.913	This study
Dihydride [FCC]	High-oxygen					
	#1	1.64	4.3487(7)	–	–	This study[c]
	#2	1.5	4.3217(4)			Ref. [6]
	Low-oxygen					
	#1	1.71	4.3506(3)	–	–	This study[c]
	#2	1.75	4.3622(6)			This study

[a] Values from absorption *P–C* isotherms on preparation.
[b] The lattice parameters a' and c' for the pseudo-cubic FCC structure were taken as $a' = \sqrt{2}(a_{BCT})$, $c' = c_{BCT}$ [6]. c'/a' is an indicator of deformation from cubic with $c'/a' = 1$.
[c] Samples were taken from the same lot as those used for SEM-EDX and *P–C* isotherms.

Two different lots were examined for each oxygen level to confirm that the difference in lattice parameters depends on oxygen concentration.

The alloy phase of the high-oxygen samples had a lattice parameter smaller by about 0.01 Å than that of the low-oxygen samples. This is because the content of Ti, which has a larger atomic size than V and Mn, decreased in the main phase as a result of formation of a Ti-rich secondary phase, as shown by the SEM–EDX results. This is consistent with our previous result indicating that decreasing Ti concentration leads to an increase in the equilibrium pressure and a decrease in the lattice parameter [8]. A significant difference between the axes ratios in the monohydride phases for the two groups was observed. The values of c'/a', corresponding to the ratio of the axis lengths in the pseudo-cubic FCC lattice, ranged from 0.94 to 0.95 for the high-oxygen samples, but was around 0.91 for the low-oxygen samples. Reducing the oxygen content results in greater deformation of the pseudo-cubic FCC lattice of the monohydride. In our previous study, where a conventional-grade V material was used, Ti-rich alloys tended to have a smaller ratio, e.g. 0.91 for $Ti_{1.2}V_{1.0}Mn_{0.8}$, and Mn-rich alloys tended to have a ratio close to or equal to 1. The result obtained in this study seems reasonable since c'/a' for the main phase in the low-oxygen sample with the richer Ti composition was smaller than the value for the high-oxygen sample. Interstitial oxygen, which has a larger atomic size than hydrogen, may tend to reduce the anisotropic deformation of the lattice, although this is difficult to confirm experimentally.

4. Discussion

The effects of oxygen in V metal and V-based BCC alloys on hydrogenation properties have already been reported. Reilly and Wiswall reported *P–C* isotherms of V–H systems and found that the dissociation pressure of the $VH_{\sim 1}$–$VH_{\sim 2}$ system was higher by a factor of >2 when the starting material was commercial-grade V containing 420 ppm oxygen instead of zone-refined V containing 112 ppm oxygen; this was clearly shown in a van't Hoff plot [9]. They also mentioned that there was no difference in the position of the phase boundaries in the system as determined from the isotherm shapes. Tsukahara et al. examined *P–C* isotherms for V containing 4000 ppm oxygen, which showed completely different curves from those for V containing 200 ppm oxygen [10]. These results indicate that the oxygen content strongly affects the *P–C* isotherms of V. The oxygen effect in V was expected to be reduced by alloying with another element with a stronger affinity for oxygen, such as Ti. Tsukahara et al. also reported oxygen effects in a V-based multicomponent alloy, $V_3TiNi_{0.56}Co_{0.14}Nb_{0.047}Ta_{0.047}$ [10]. They indicated that part of the oxygen was taken into a secondary phase such as Ti_4Ni_2O, which reduced the oxygen content in the main phase. Similar phenomena are often observed in Ti-containing V alloys; for example Komaki et al. reported that the oxygen effect was smaller in (Ti–V)–H systems than in the V–H system because oxygen reacts with Ti and precipitates a secondary phase, which eventually reduces the oxygen content in the mother phase [13].

As the previous reports suggested, we need to discuss two possibilities for oxygen effects on *P–C* isotherms. One is an effect essentially caused by oxygen solved in the main phase (the *primary* effect). This has been observed as a significant effect in pure V, and can also be observed in V-containing BCC alloys. The other is formation of the secondary phase promoted by the presence of oxygen, which results in changes in the composition of the main phase (the *secondary* effect), as observed in V-containing alloys.

The *P–C* isotherms obtained in this study indicated that a higher concentration of oxygen in the alloy significantly affects the pressures of the higher plateaus corresponding to formation and dissociation of the dihydride. The position of the boundary between the dihydride region and the adjacent plateau region did not change significantly. These results largely agree with those observed in the desorption *P–C* isotherms for the V–H system reported by Reilly and Wiswall [9]. Our results, however, include two more points that have not been highlighted. The effect of increasing the plateau pressure was greater in absorption than in desorption. The equilibrium pressures of the high-oxygen sample were higher than those of the low-oxygen sample by a factor of 5–7 for absorption and ~2 for desorption. The other point is that the oxygen effect was not observed for the lower plateau corresponding to formation and dissociation of the monohydride. The significant difference in the oxygen effect between the formation of the dihydride and the monohydride is probably related to the difference in hydrogen occupation sites and local deformation of the lattice. This corresponds to the *primary* oxygen effect.

The effects of oxygen on hydrogen solubility in V have been reported, but most reports focus on the region of dilute hydrogen concentration, up to several atomic percent. The literature states that oxygen atoms are known to occupy O sites in the BCC lattice

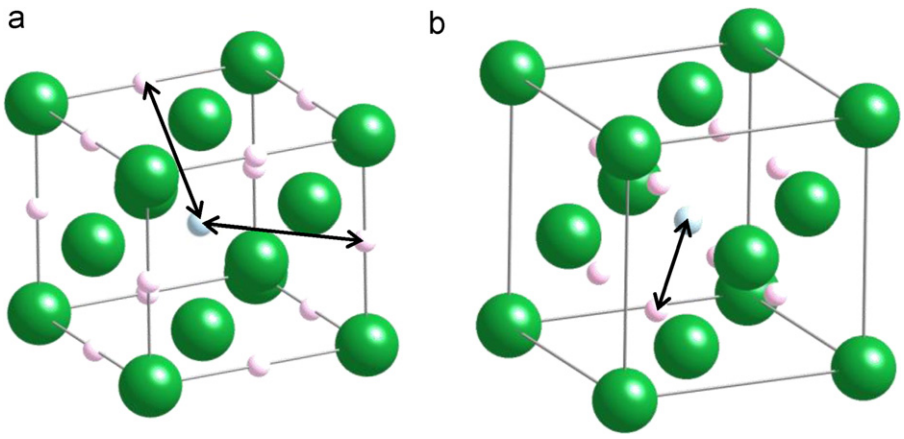

Fig. 7. Relationship between the location of hydrogen and oxygen atoms in the lattice of the monohydride (a) and dihydride (b). Oxygen atoms are placed in the body-center position; it is assumed that they occupy octahedral sites in the FCC lattice. Hydrogen atoms occupy octahedral sites in the monohydride and tetrahedral sites in the dihydride.

and to trap hydrogen atoms [14]. Solved oxygen has the effect of increasing the limit of hydrogen solubility by preventing precipitation of a hydride phase. There are few reports describing the oxygen effect on hydride phase formation. Given that oxygen atoms are much larger than hydrogen atoms (the empirical atomic radii are 0.25 Å for hydrogen and 0.60 Å for oxygen [15]), oxygen atoms will tend to occupy larger interstitial sites in the metal lattice of hydride phases. This suggests that oxygen atoms will also occupy O sites in the FCC metal lattice. In the monohydride phase, both hydrogen and oxygen would occupy O sites (Fig. 7a). Hydrogen occupation would be partly blocked by oxygen atoms, but the blocking itself would have little effect on the total hydrogen capacity because the concentration of oxygen is only 1.67 at.% in this case. Interaction between oxygen and hydrogen will be limited since they are separated by a sufficiently great distance: 2.72 Å and 2.90 Å for the high-oxygen sample, compared with the observed shortest O–H distance of ~2.6 Å previously reported for hydrogenation of oxygen-stabilized η-$Zr_3V_3O_x$ [16]. The lattice deformation may be locally generated around each oxygen atom, which affects hydrogen occupation, but it will be also limited, considering the oxygen content. Therefore, the oxygen effect in the formation of the monohydride is likely to be small. In the dihydride with a CaF_2-type structure, hydrogen occupies T sites in the FCC lattice. Because of the close proximity of the O site and the T site (Fig. 7b, 1.88 Å for the high-oxygen sample), hydrogen occupation will be affected more strongly than in the monohydride as a result of direct interaction between oxygen and hydrogen, and of local lattice deformation induced by oxygen. Blocking of the T sites by oxygen atoms located at the adjacent O sites can explain a small decrease in capacity, i.e. by a maximum of 0.134 H/M [=1.67 at.% × 8 (the coordination number of H to O)], but this cannot explain the increase in the equilibrium pressure. A possible explanation is that the electron densities at hydrogen sites are increased by electrons brought by oxygen, and this raises the heat of solution of hydrogen [17]. It is still an open question as to why the effect is not limited locally but affects all of the hydrogen sites, as suggested by the shift of the whole of the plateau to a higher pressure. The rapid increase in the slope in the plateau on the high hydrogen content side observed in the high-oxygen sample may imply a local oxygen effect.

The observed results may be partly attributed to changes in the mechanical properties of the alloys and the hydrides. Some reports have indicated that the lattice parameter and hardness of V increase with increasing oxygen content [18,19]. Bradford et al. reported that V metal loses ductility and become brittle at −125 °C for oxygen concentrations of 1500–2000 ppm. Actually, the V metal with the lower oxygen concentration which we used was so ductile that a piece of it was easily flattened by hammering. In contrast, a piece of the V metal with the higher oxygen concentration was easily broken by hammering. This difference affects the ductility of the two Ti–V–Mn samples. In general, hydride formation is accompanied by large lattice expansion and deformation, so that, inevitably, the mechanical properties will be related to hydrogenation properties. It is known that lattice defects such as dislocations are introduced upon hydrogenation [20–24], and that defect formation is related to pressure hysteresis [23–25], as reported for $LaNi_5$. Changes in the mechanical properties due to solved oxygen possibly contribute to increasing formation energy of defects and result in increasing hysteresis in *P–C* isotherms.

The *secondary* oxygen effect is accompanied by formation of the secondary phase, as observed in Ti-containing V alloys [13]. In the high-oxygen sample used in this study, the formation of the Ti-rich phase induced a shift of the composition of the main phase to Ti-poor and V-rich, which reduced the lattice parameter by 0.01 Å (Table 3). The equilibrium absorption pressures of the two samples differ by a factor of at most 6.7, as described in Section 3.2. Equilibrium pressures are generally so sensitive to the lattice parameter in BCC alloys that even a small change in the lattice parameter provides a significant difference in the equilibrium pressure. For example, in the reports on composition dependence of Ti–V-based BCC alloys, a difference in the lattice parameter of about 0.01 Å changed the equilibrium pressure by a factor of ~1.4 in Ti–V–Cr [1], and by a factor of 3–6 in Ti–V–Mn [8]. The secondary oxygen effect caused by small changes in the composition and the lattice parameter is therefore likely to be appreciable in Ti–V-based BCC alloys, as well as the primary effect.

5. Conclusion

The hydrogenation properties of Ti–V–Mn alloys showing two plateaus in their *P–C* isotherms were studied for two samples containing 0.530 mass% and 0.051 mass% of oxygen, respectively. A significant oxygen effect was observed as an increase in the pressure of the higher plateau, which resulted in positive shifts in the formation and dissociation enthalpies of the dihydride. However, there was no significant difference between the two samples with respect to the hydrogen capacity, the phase boundaries on the *P–C* isotherms, or the formation enthalpy of the monohydride. In conclusion, increasing oxygen concentration induces a change in the formation enthalpy of the dihydride through the following two effects: oxygen solved in the main phase affects hydrogen occupation directly (the primary effect), and formation of a Ti-rich secondary phase changes the composition and the lattice parameter of the main phase (the secondary effect).

Acknowledgement

This work was supported by The New Energy and Industrial Technology Development Organization (NEDO) under "Advanced Fundamental Research on Hydrogen Storage Materials (HYDRO-STAR)."

References

[1] E. Akiba, H. Iba, Intermetallics 6 (1998) 461.
[2] M. Okada, T. Kuriiwa, T. Tamura, H. Takamura, A. Kamegawa, J. Alloys Compd. 330–332 (2002) 511.
[3] K. Iwase, Y. Nakamura, K. Mori, S. Harjo, T. Ishigaki, T. Kamiyama, E. Akiba, J. Alloys Compd. 404–406 (2005) 99.
[4] D. Mori, K. Hirose, K. Komiya, M. Ishikiriyama, N. Haraikawa, K. Toh, K. Fujita, S. Watanabe, M. Miyahara, S. Mikuriya, M. Tsukahara, Abstract of International Symposium on Metal–Hydrogen Systems (MH2008), Reykjavik, Iceland, June 24–28, 2008.
[5] H. Iba, E. Akiba, J. Alloys Compd. 231 (1995) 508.
[6] Y. Nakamura, E. Akiba, J. Alloys Compd. 311–312 (2000) 317.
[7] Y. Nakamura, E. Akiba, J. Alloys Compd. 316 (2001) 284.
[8] Y. Nakamura, E. Akiba, J. Alloys Compd. 345 (2002) 175.
[9] J.J. Reilly, R.H. Wiswall Jr., Inorg. Chem. 9 (1970) 1678.
[10] M. Tsukahara, K. Takahashi, A. Isomura, T. Sakai, J. Alloys Compd. 265 (1998) 257.
[11] http://homepage.mac.com/fujioizumi/.
[12] F. Izumi, T. Ikeda, Mater. Sci. Forum 321–324 (2000) 198.
[13] M. Komaki, C. Nishimura, M.J. Amano, Jpn. Inst. Metal 56 (1992) 729.
[14] Y. Fukai, The Metal-hydrogen Systems, vol. 21, Springer Series in Material Science, Springer, Berlin, 1993 (Chapter 4).
[15] J.C. Slater, J. Chem. Phys. 41 (1964) 3199.
[16] I.Yu. Zavaliya, W.B. Yelonb, P.Y. Zavalijc, I.V. Saldana, V.K. Pecharsky, J. Alloys Compd. 309 (2000) 75, and the references cited.
[17] J.K. Nørskov, Phys. Rev. B: Condens. Matter Mater. Phys. 26 (1982) 2875.
[18] S. Beatty, Trans. AIME J. Met. (September) (1952) 987.
[19] A. Bradford, O.N. Carlson, Trans. ASM 55 (1962) 169.
[20] Y. Nakamura, E. Akiba, J. Alloys Compd. 308 (2000) 309.
[21] R. Černý, J.-M. Joubert, M. Latroche, A. Percheron-Guégan, K. Yvon, J. Appl Crystallogr. 33 (2000) 997.
[22] Y. Shirai, H. Araki, T. Mori, W. Nakamura, K. Sakaki, J. Alloys Compd. 330–332 (2002) 125.
[23] H. Inui, T. Yamamoto, M. Hirota, M. Yamaguchi, J. Alloys Compd. 330–332 (2002) 117.
[24] K. Sakaki, E. Akiba, M. Mizuno, H. Araki, Y. Shirai, J. Alloys Compd. 473 (2009) 87.
[25] J. Matsuda, Y. Nakamura, E. Akiba, Abstract of MRS Fall Meeting 2009, Boston, USA, November 30–December 4, 2009, W8.17.